Multiple phase structures of $NiSi_2$ on Si(001): An atomic view

Y. Khang and Y. Kuk
Department of Physics, Seoul National University, Seoul 151-742, Korea
(Received 3 November 1995)

Three different growth structures of nickel silicide on the Si(001) were observed as functions of coverage and temperature. The structure of (2×1) Si dimer bonds is formed at the interface before a bulklike (1×1) structure is grown. The (2×1) and (1×1) structures coexist at the coverage of less than 1 ML. The (1×1) structure contains many twin boundaries that can be developed into ''facetbars'' in a thicker film. High-temperature annealing induces a $(\sqrt{2}\times\sqrt{2})$-$R45°$ structure with metallic character. Conflicting results in macroscopic Schottky barrier height measurements can be explained by coexistence of these three observed phases.

I. INTRODUCTION

Metal silicides are technologically important in semiconductor device fabrication because of their low sheet resistances, abrupt interfaces with strong bonds.[1–5] Nearly perfect epitaxial silicides can be grown on various silicon surfaces and their applications to high-density integrated circuits have been tried. Metal silicides reveal Schottky barrier heights (SBH's) that vary from nearly Ohmic contact to more than 1 eV. The mechanism and origin of SBH's are not well understood in spite of intensive studies for the past two decades.[6–8] Until recent years, Fermi-level pinning has been most widely accepted for the formation mechanism.[9–11] In this model, defects or gap states induced by the metal in the semiconductor-metal interface pin the Fermi level of a semiconductor at the interface to satisfy the charge neutrality. Recently it was experimentally proved that an SBH can be determined by the local atomic structure of the metal-semiconductor interface.[12] The development of the epitaxial growth technique enables the control of the grown layer with atomic precision. The ''template method,'' developed for the epitaxial growth of $NiSi_2(111)$ layers on Si(111) not only produces an atomically sharp interface but also controls the stacking sequence at the interface.[13] In the $NiSi_2$/Si(111) system, a selectively grown interface without the stacking fault at the interface (A type) reveals an SBH of 0.65 eV while one with the stacking fault (B type) reveals that of 0.79 eV.[12,14] Correlation between the interface structure and SBH becomes one of the most important topics in semiconductor science.

For epitaxially grown $NiSi_2(100)$ on the Si(100), there were conflicting results on measured SBH with varying dopant density in the substrate and growing condition.[15] It was reported that low-temperature annealing (<450 °C) after Ni and Si codeposition induces macroscopic ''facet bars'' aligned along the [110] with (111) facets,[16] and these samples show the SBH of 0.65 eV, similar to that of A type interface in $NiSi_2$/Si(111) for an n-type Si substrate.[15] After annealing over 700 °C, a uniform interface without the facet bar reveals a low SBH of 0.4 eV. These conflicting results are interpreted as a proof of the local atomic structural dependence of the SBH. For a p-doped substrate, the variation of SBH was explained by the presence of a reconstruction at the interface. The interfacial (2×1) reconstruction was first reported in the $CoSi_2$/Si(100) system from the transmission electron microscopy (TEM) diffraction pattern.[17] A similar (2×1) streak pattern was observed in the $NiSi_2$/Si(100) system, suggesting a similar interface reconstruction.[18] The driving force of the interface reconstruction was explained by the dimerization of Si dangling bonds at the interface with sixfold coordination of Ni atoms[17,18] as shown in Fig. 1. However, the correlation between varying SBH and the reconstruction has not been understood yet.

The surface structure of the $NiSi_2(001)$ was previously studied by a scanning tunneling microscope (STM) on a silicide surface cleaned by sputtering and annealing.[19] It is not clear if the structure of the sputtered and annealed surface is the same as that of an epitaxially grown sample. But the growth structure as a function of coverage can only be studied with the latter sample. The structures of thick epitaxially grown layers were also studied by low-energy ion scattering[20] (LEIS) and low-energy electron diffraction (LEED).[21] It was suggested in the STM study[19] that the surface was terminated by an additional Si atomic layer on T_4 sites (on-top sites) and regularly spaced Si adatoms on H_4 sites (hollow sites), forming a $\sqrt{34}\times\sqrt{34}$ structure. At the

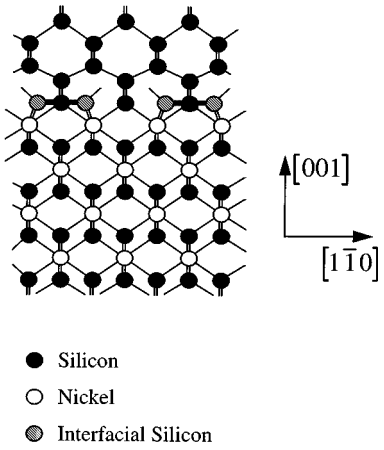

FIG. 1. A schematic diagram of the $NiSi_2$/Si(001) interface. The interfacial Si layer can be dimerized to decrease the interfacial energy.

patch patterns, which were arranged to form the superstructure, Si adatoms were assigned to be situated on top of the H_4 site. The presence of defects was also proposed in the LEED study to explain the higher-order spots and the *I-V* data. An LEIS study, however, suggested a model with additional Ni layers or many missing Si adatoms, contrary to LEED and STM studies. In a recent TEM study, it was found that formation of twin boundaries was energetically favorable on an annealed epitaxial $NiSi_2(001)$ film.[22] In a calcium fluorite structure, it is understood that a twin boundary made of two hcp stacking faults is not energetically costly. In spite of these studies, the atomic arrangements of the super structures are still not understood.

In this paper, we report three different growth structures of the nickel silicide on Si(001) at several temperatures and coverages. The (2×1) Ni adsorbed layer is formed at the early stage of growth with sixfold coordination of Ni at the interface; thus the nickel-induced phase has been observed between $NiSi_2$ phase islands. The (2×1) structure observed in the TEM diffraction pattern can be explained by the present STM observation. The (1×1) islands are formed on top of the (2×1) structure with many twin boundaries. We propose a new model for the (1×1) island formation. The observed superstructure is not made of an adsorbed layer of 1 ML thin but multilayer deep twin boundaries. High-temperature annealing produces a $(\sqrt{2}\times\sqrt{2})$-$R45°$ structure that has not been observed so far to our knowledge. It is concluded that the conflicting results in Schottky barrier height measurements are caused by the multiple phases of $NiSi_2$ structure grown on the Si(001).

II. EXPERIMENT

The experiment was performed by using a UHV STM. The detailed design of the STM used in this study can be found elsewhere.[23] An As-doped Si wafer (resistivity of 2–5 Ω cm) was prepared by Shiraki cleaning[24] in order to obtain a clean dry oxide layer before being introduced into the UHV STM chamber. The sample was outgassed at ~600 °C for several hours, then flashed at 1250 °C and cooled slowly afterwards. A sharp (2×1) pattern could then be obtained without trace of impurity. A small *e*-beam deposition source was used to deposit Ni with a typical deposition rate of 2 ML/min. The coverage was calibrated by a combination of Auger electron spectroscopy, STM images, secondary ion mass spectrometry, and Rutherford backscattering. The $NiSi_2$ layer was grown on the Si(001) substrate by deposition of Ni and subsequent annealing at 350–750 °C. A new substrate was introduced for each coverage in order to minimize the effect that early growth structure may influence the structure at subsequent coverages. Several silicide structures were observed at various coverages and annealing temperatures. Since some are metastable structures, equilibrium structures within the annealing temperature of 350–750 °C and the coverage of 0–5 ML are only reported here. Scanning tunneling spectroscopy (STS) was used to determine the surface electronic structure of the silicide structures.

III. RESULT AND DISCUSSION

From earlier studies, it has been known at the early stage of Ni deposition that Ni diffuses into the bulk of Si(001) and forms a $(2\times n)$ structure in addition to the original (2×1).[25] Metal atoms diffuse into the bulk of Si while Si atoms diffuse out toward the surface, but the diffusion rate varies for different metals. Therefore, the diffusion rate and the misfit between the metal silicide and Si are the determining factors for the structure of epitaxial silicide. At the Ni coverage of $\leq$0.2 ML, the $(2\times n)$ structure induced by metal in-diffusion was observed, mainly a (2×8) structure. The size of patches with superstructure was increased with increasing Ni coverages. But, there was no trace of Ni-induced protrusions or adatoms even after annealing at 350–750 °C. At the coverage of 0.2–0.5 ML, the Ni-induced row began to appear, aligned along the $\langle110\rangle$ directions with budlike features protruding from the row (Fig. 2). After the sample was annealed at >400 °C, the budlike feature disappeared and newly formed rows remained. As the coverage exceeds 0.5 ML, the added row aggregated to form a new

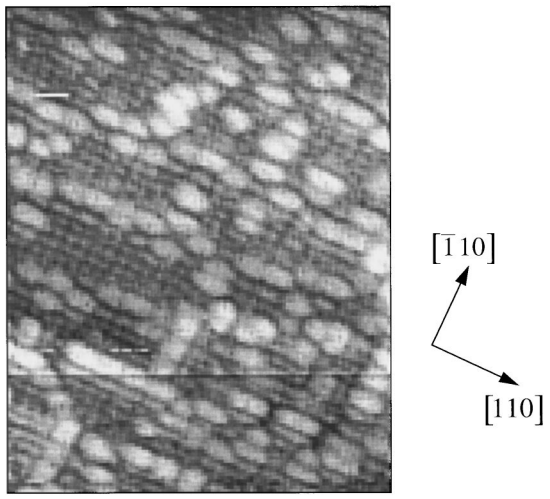

FIG. 2. An 80×105-Å^2 STM image at Ni coverage of $\leq$ 0.2 ML on Si(001). Budlike Ni-induced features are protruded from Si-(2×1) rows.

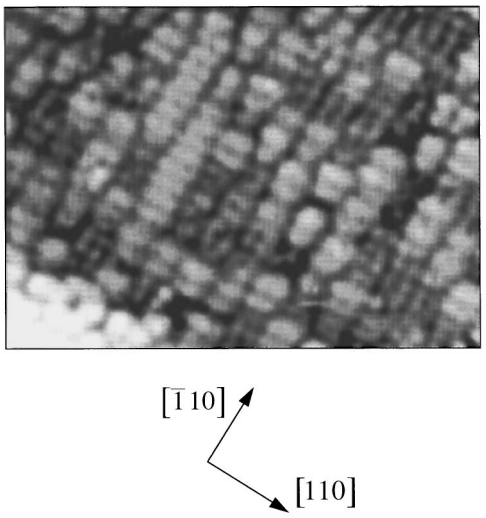

FIG. 3. A 75 × 55-Å^2 STM image of Ni-induced (2×1) at the Ni coverage of ~0.5 ML. Budlike features at Ni coverage of $\leq$0.2 ML were aggregated to form a new Ni-induced (2×1) phase with increasing Ni coverage.

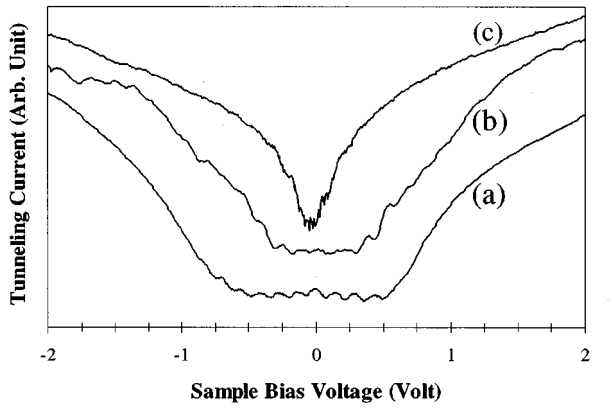

FIG. 4. The *I*-*V* characteristics on partially covered nickel silicide surface; (a) on top of the Si substrate, (b) a Ni-induced (2×1) row, and (c) (1×1) island, respectively. (a) and (b) show the band gap of $\sim$1.1 eV (band gap of Si) and $\sim$0.7 eV, and (c) shows no band gap.

(2×1) phase (Fig. 3). From the observed images only, it is difficult to determine whether the added rows are made of Ni or Si layers. But it is noticeable that the dimers induced by the added row appear wider than those on the Si substrate, as shown in Fig. 3. In order to verify the chemical identity of the rows, STS was performed. On top of defect-free Si-(2×1), the band gap of 1.1 eV was observed, while it was $\sim$ 0.7 eV on top of the added row of (2×1) structure, as shown in Fig. 4. The lower band gap clearly indicates that the new (2×1) layer induced by the added row shows different semiconducting character but they are not metallic. The structure and growth mechanism at early stage can be proposed from the observed (2×1) structure. As a Ni atom arrives at the Si(001)-(2×1) surface, it prefers to have sixfold coordination with Si. In the absence of the top Si layer (Fig. 1), it only has fivefold coordination and the Si atom with dangling bond under the Ni atom can dimerize to lower the interfacial energy. Two neighboring Ni atoms appear as a dimer but their voltage dependence is different from that of

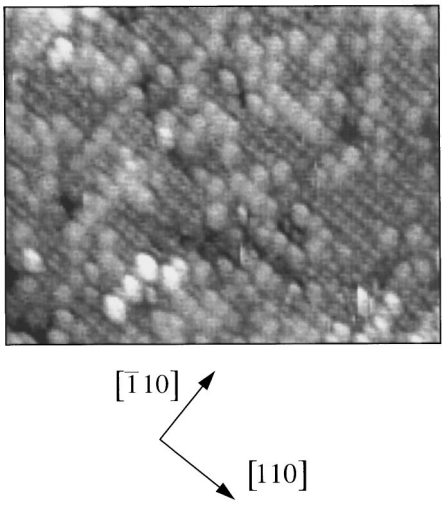

FIG. 5. A 125×100-Å^2 STM image. Fully developed Ni-induced (2×1) structure. The second layer of the Ni-induced (2×1) chain structure begins to grow.

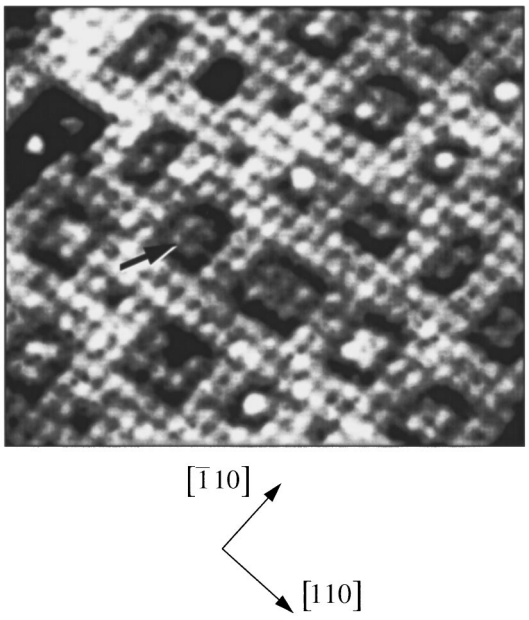

FIG. 6. A 130×110-Å^2 STM image of the $NiSi_2$-(1×1) island. The patch structures of 2×2, 2×3, and 1×1 are surrounded by bulklike 1×1 structure.

the Si dimer. Two Ni rows appear to be shifted toward each other by 1/2 of 2.8 Å as shown in Figs. 1 and 5. The geometric and electronic structure of the Ni-induced (2×1) layer can be understood further with the theoretical calculation.

At a coverage of >0.7 ML, rectangular patches of islands with 3–4 ML high and aligned along the $\langle110\rangle$ directions began to appear. After annealing the sample at 350–650 °C, this surface appears as a good metal as shown in Fig. 4. The distance between nearest neighbors on the island is 3.8 Å, exactly the same as that in bulk $NiSi_2$. The surface can be interpreted as the metal-terminated $NiSi_2$ with the height of 3 ML, but Si-terminated layers appeared rarely

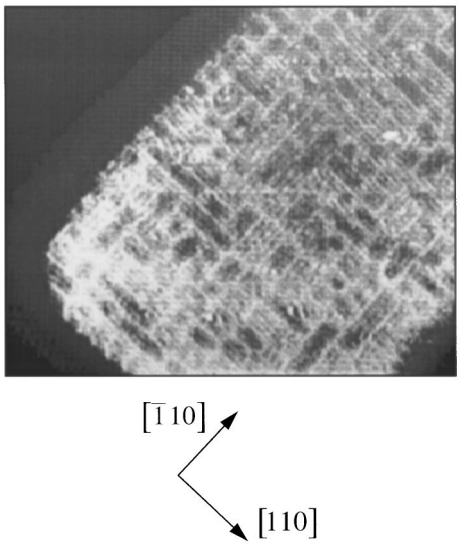

FIG. 7. A 250×200-Å^2 STM image. With increasing Ni coverage, 2×2 patches on the $NiSi_2$-(1×1) island are more regularly arranged.

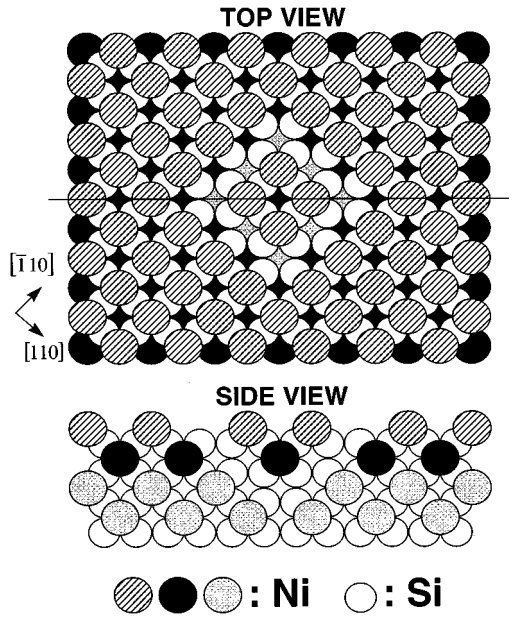

FIG. 8. Model of patch on $NiSi_2$-(1×1) island. In side view, the inverse-pyramidal structure of the patch is proposed.

with the height of 4 ML. The surface contains patch patterns, which can be arranged regularly after annealing at 600 °C for several hours. This superstructure was previously reported as $\sqrt{34}\times\sqrt{34}$ interpreted as added Si atoms at H_4 sites while other atoms are Si atoms on top of T_4 sites. By annealing the sample for lower temperature or shorter period, many patches with varying sizes, mainly 2×2 or occasionally 2×3, 2×1, and 1×1 structure, are surrounded by the (1×1) $NiSi_2$ matrix structure as shown in Fig. 6. The atomic arrangement (shown by an arrow) and scanning tunneling spectroscopic results within the patches are the same as that

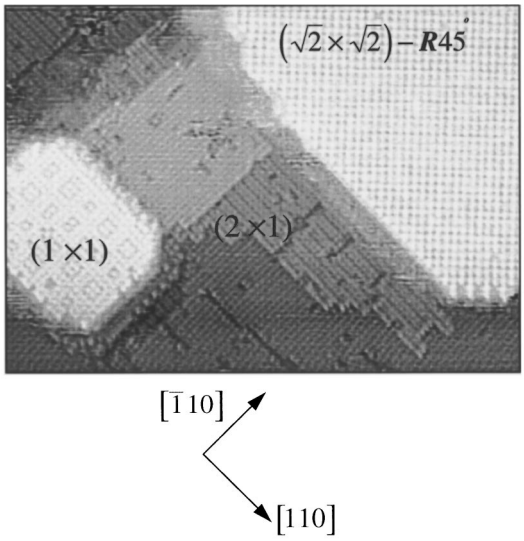

FIG. 9. A 320×230-Å^2 STM image of Ni silicide on the Si(001) surface. A $(\sqrt{2}\times\sqrt{2})$-$R45°$ structure appeared after annealing of >650 °C). Three different phases of the (1×1) patch structure, the (2×1) chain structure, and the $(\sqrt{2}\times\sqrt{2})$-$R45°$ structure were visible in an image.

on bulk termination but shifted by 1.9 Å. We suggest that these patches on the (1×1) structure island are originated from stacking faults during the formation of the island. Therefore, these patches have inverse pyramidal structure. For much increased Ni coverage, the patches on the island grow along the $\langle110\rangle$ directions (Fig. 7). It was reported in the TEM study that the twin boundary (two fcc-hcp-fcc stackings) can be formed easily in a $NiSi_2$ bulk and is not energetically costly.[26] This inverse pyramidal structure in Fig. 8 can be seen as a twin boundary, since two hcp stacking faults can be found if the structure is cut along the (100). Since the height of the pyramid is limited by the film thickness, the 2×2 unit, which is the base unit of the $(\sqrt{34}\times\sqrt{34})$ reconstruction, is the most favorable for the Ni

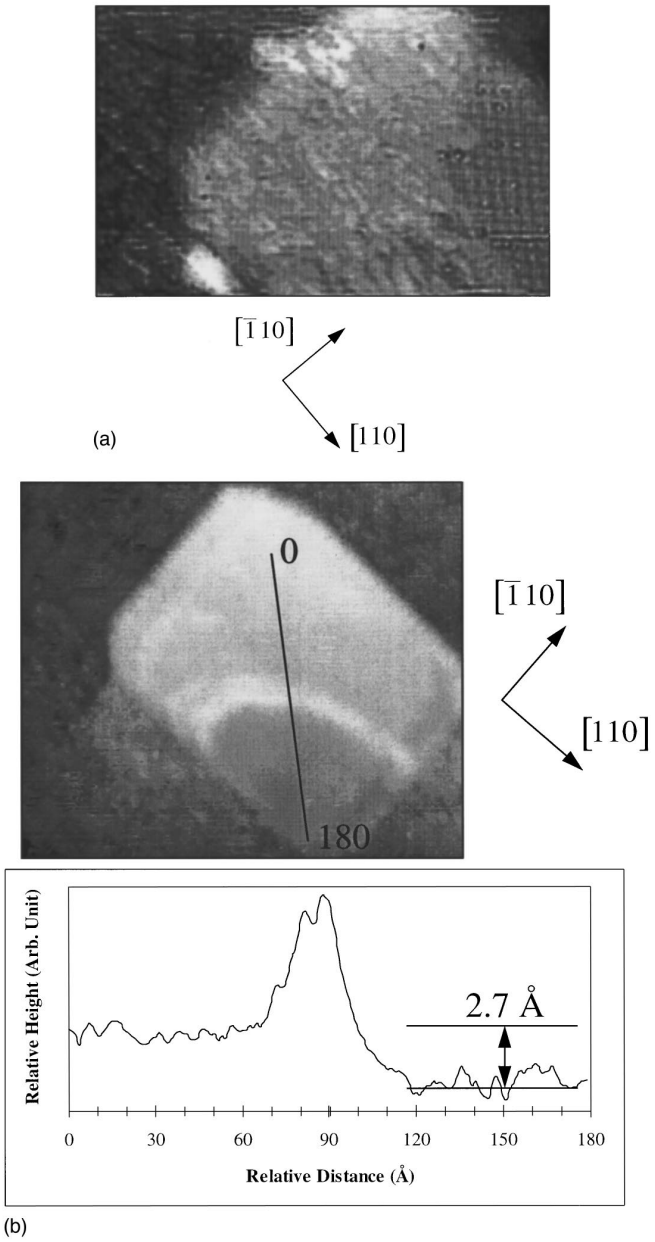

FIG. 10. STM images of 150×90 Å^2 for (a) and of 150×130 Å^2 for (b). Partially ordered structure can be seen, as shown in (a) and (b). Higher Ni atomic density is observed between the ordered and disordered parts, as shown in (b).

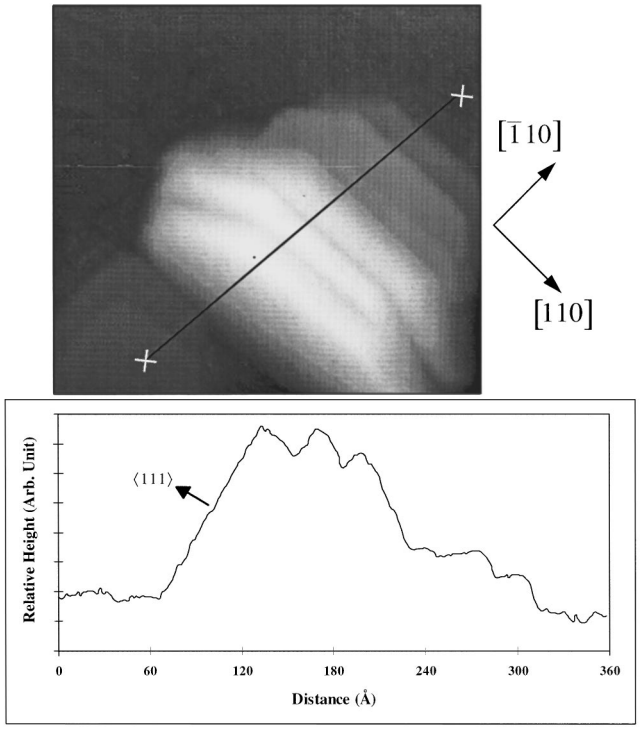

FIG. 11. A 370×340-Å^2 STM image, with a (111) faceted $NiSi_2$ island and a cross-sectional view. In a cross-sectional view, the (111) direction is indicated by the arrow.

thickness used in our experiment. The twin boundary between $NiSi_2$ layers causes a detrimental defect to cause conflicting SBH results. The macroscopic patches on the $NiSi_2$ overlayer have been observed in the plan view TEM,[16] where the patches were called ''facet bars.'' The (1×1) islands observed in our experiment can be identified as the nucleation sites of the facet bars. From the earlier experimental results of cross-sectional TEM,[16] the facet bar shows (111) direction faceting between the $NiSi_2$ overlayer and Si substrate embedded into the Si substrate. The shape of the interface under the island can be further studied by ballistic electron emission microscopy.

The (1×1) islands separated by the (2×1) adlayer were also observed earlier by TEM.[16] From plan view TEM, the same island formation as the present study was observed but those islands were assumed to be separated by a bare Si layer, called ''coreless dislocation.'' In this study, it was found that the (1×1) islands are separated by the Ni-induced (2×1) adlayer. The islands formed on the upper and lower terraces separated by a single atomic height step are shifted by a displacement of $a/4\langle111\rangle$, the Ni-Si interatomic bond length. Therefore, the dislocation with Burgers vector of $a/4\langle111\rangle$ has to be formed for two islands to coalesce to single island. In the low-temperature regime, an atomic step works as a barrier for the (1×1) island to grow.

At higher annealing temperature $>650\,^\circ$C, the third structure was observed. After annealing at the higher temperature, the (1×1) island structure began to disappear. A new $(\sqrt{2}\times\sqrt{2})$-$R45^\circ$ structure began to grow and cover extensive area as shown in Fig. 9. One can imagine Ni further diffuses into the bulk Si and the stoichiometry of the surface is broken. However, the detailed composition is not clearly known yet, since they always coexist with the (1×1) structure. By annealing at higher temperature, since Ni in-diffuses further only the $(\sqrt{2}\times\sqrt{2})$-$R45^\circ$ phase and the (2×1) adsorbed phase can be observed.

The fully ordered island can be formed by annealing the sample for more than 1 h at $>450\,^\circ$C. When the sample was annealed for a shorter period, for example, less than 30 min, partially ordered islands could be obtained. Figure 10 shows one of partially ordered silicide islands. The silicide island is formed by in-diffusion of adsorbed Ni atoms and out-diffusion of substrate Si atoms, followed by the formation of $NiSi_2$. Noncrystalline Ni is separated from the $NiSi_2$ by higher Ni atomic density as shown in the cross-sectional view of the island in Fig. 10. Well-ordered (1×1) area was separated by a diffusion barrier where the stoichiometry between Ni and Si was not 1:2.

By annealing at the temperature of $>700\,^\circ$C, faceting along (111) is often observed (Fig. 11). The (111) direction faceting outward from the surface was also reported in the earlier TEM results.[18] But, it is not clear whether this faceting is extended to the (111) interface since the interfacial energy of $NiSi_2$/Si(111) is lower than that of $NiSi_2$/Si(001). It was also known that the surface energy of the $NiSi_2$(111) interface is lower than that of the $NiSi_2$(001). Therefore, there are two possibilities; surface faceting and faceting at the interface. In the earlier electrical measurement,[15] the SBH on the (100) was close to that on the *A* type $NiSi_2$/Si(111) for some samples. It is possible that some parts of this surface are covered with a phase with lower SBH, which will determine the measured value in the macroscopic measurement.

IV. CONCLUSION

We observed three different structures of the nickel silicide on Si(100) surface at several temperatures and coverages. A Ni-induced (2×1) adsorbed layer is formed at the early stage of growth. The structures is induced by the dimerization of Si dangling bonds under the top Ni layer. The (1×1) islands are formed on top of the (2×1) structure with many twin boundaries. The twin boundaries may work as nucleation sites of the previously observed facet bar. At high temperature, $>650\,^\circ$C, a $(\sqrt{2}\times\sqrt{2})$-$R45^\circ$ structure caused by in-diffusion of Ni into Si was observed. The multiple phases on the nickel silicide layer grown on the Si(100) surface can cause the conflicting results in SBH measurements.

ACKNOWLEDGMENTS

This work was supported in part by the Korea Science and Engineering Foundation through the Science Research Center (1996) and Korean Ministry of Education (BSRI-95-2416).

[1] D. Cherns, G.R. Anstis, J.L. Hutchison, and J.C.H. Spence, Philos. Mag. A **46**, 849 (1982).
[2] R.T. Tung, J. Vac. Sci. Technol. A **7**, 598 (1989).
[3] J. Derrien and F. d'Avitaya, J. Vac. Sci. Technol. A **5**, 2111 (1987).
[4] J.M. Gibson, J.C. Bean, J.M. Poate, and R.T. Tung, Appl. Phys. Lett. **41**, 818 (1982).
[5] E. Rosencher, S. Delage, F.A. d'Avitaya, and O.K. Anderson, in *Metallization and Metal-Semiconductor Interfaces*, edited by I.P. Batra (Plenum, New York, 1988).
[6] E.H. Rhoderick and R.H. Williams, *Metal-Semiconductor Contacts* (Clarendon, Oxford, 1988).
[7] L.J. Brillson, Surf. Sci. Rep. **2**, 123 (1982).
[8] W.E. Spicer, N. Newman, T. Kendelewicz, W.G. Petro, M.D. Williams, C.E. McCants, and I. Lindau, J. Vac. Sci. Technol. B **3**, 1178 (1985).
[9] W. Mönch, J. Vac. Sci. Technol. B **6**, 1270 (1988).
[10] W. Walukiewicz, Phys. Rev. B **37**, 4760 (1988).
[11] J. Tersoff, Phys. Rev. Lett. **52**, 465 (1984).
[12] R.T. Tung, Phys. Rev. Lett. **52**, 461 (1984).
[13] R.T. Tung, J.M. Gibson, and J.M. Poate, Phys. Rev. Lett. **50**, 429 (1983).
[14] R.J. Hauenstein, T.E. Schlesinger, T.C. McGill, B.D. Hunt, and L.J. Schowalter, J. Vac. Sci. Technol. A **4**, 860 (1986).
[15] R.T. Tung, A.F.T. Levi, J.P. Sullivan, and F. Schrey, Phys. Rev. Lett. **66**, 72 (1991).
[16] J.L. Batstone, J.M. Gibson, R.T. Tung, and A.F.J. Levi, Appl. Phys. Lett. **52**, 828 (1988).
[17] D. Lorretto, J.M. Gibson, and S.M. Yalisove, Phys. Rev. Lett. **63**, 298 (1989).
[18] J.P. Sullivan, R.T. Tung, and F. Schrey, J. Appl. Phys. **72**, 478 (1992).
[19] R.S. Becker, A.J. Becker, J. Sullivan, and R.T. Tung, J. Vac. Sci. Technol. B **11**, 752 (1993).
[20] J.H. Huang, R.S. Daley, D.K. Shuh, and R.S. Williams, Surf. Sci. **186**, 115 (1987).
[21] S.C. Wu, Z.Q. Wang, Y.S. Li, and F. Jono, Solid State Commun. **57**, 687 (1986).
[22] I. Kunishima, K. Suguro, T. Aoyama, and J. Matsunaga, Jpn. J. Appl. Phys. **29**, L2329 (1990).
[23] Y. Kuk and P.J. Silverman, Rev. Sci. Instrum. **60**, 165 (1989).
[24] A. Ishzuka and Y. Shiraki, J. Electrochem. Soc. **133**, 666 (1986).
[25] H. Niehus, U.K. Köhler, M. Copel, and J.E. Demuth, J. Microsc. **152**, 735 (1988).
[26] H. Yang, R.F. Pinizzotto, L. Luo, and F. Namavar, Appl. Phys. Lett. **62**, 2694 (1993).